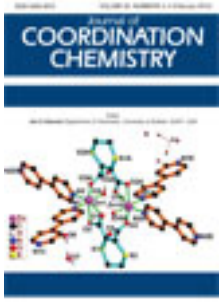

Journal of Coordination Chemistry
Publication details, including instructions for authors and subscription information:
http://www.tandfonline.com/loi/gcoo20

Synthesis and structure of a Ni(II) complex with N′,N′²-bis[(1E)-1-(2-quinolyl)methylene]propanedihydrazide: multiple intramolecular CH···π interactions between quinoline and quinolineimine chelate

Božidar Čobeljić [a], Beata Warżajtis [b], Urszula Rychlewska [b], Dušanka Radanović§ [c], Vojislav Spasojević [d], Dušan Sladić [a], Rabia Eshkourfu [a] & Katarina Anđelković [a]

[a] Faculty of Chemistry, University of Belgrade, Studentski trg 12-16, 11000 Belgrade, Serbia

[b] Faculty of Chemistry, A. Mickiewicz University, Grunwaldzka 6, 60-780 Poznań, Poland

[c] Institute of Chemistry, Technology and Metallurgy, University of Belgrade, Njegoševa 12, P.O. Box 815, 11000 Belgrade, Serbia

[d] Institute of Nuclear Sciences 'Vinča', Condensed Matter Physics Laboratory, P.O. Box 522, 11001Belgrade, Serbia

Published online: 07 Feb 2012.

To cite this article: Božidar Čobeljić, Beata Warżajtis, Urszula Rychlewska, Dušanka Radanović§, Vojislav Spasojević, Dušan Sladić, Rabia Eshkourfu & Katarina Anđelković (2012) Synthesis and structure of a Ni(II) complex with N′,N′²-bis[(1E)-1-(2-quinolyl)methylene]propanedihydrazide: multiple intramolecular CH···π interactions between quinoline and quinolineimine chelate, Journal of Coordination Chemistry, 65:4, 655-667, DOI: 10.1080/00958972.2012.658778

To link to this article: http://dx.doi.org/10.1080/00958972.2012.658778

Journal of Coordination Chemistry
Vol. 65, No. 4, 20 February 2012, 655–667

Synthesis and structure of a Ni(II) complex with N',N'^2-bis[(1*E*)-1-(2-quinolyl)methylene]propanedihydrazide: multiple intramolecular CH $\cdots$ π interactions between quinoline and quinolineimine chelate

BOŽIDAR ČOBELJIĆ†, BEATA WARŻAJTIS‡, URSZULA RYCHLEWSKA‡, DUŠANKA RADANOVIĆ§, VOJISLAV SPASOJEVIĆ¶, DUŠAN SLADIĆ†, RABIA ESHKOURFU† and KATARINA ANĐELKOVIĆ*†

†Faculty of Chemistry, University of Belgrade, Studentski trg 12-16, 11000 Belgrade, Serbia
‡Faculty of Chemistry, A. Mickiewicz University, Grunwaldzka 6, 60-780 Poznań, Poland
§Institute of Chemistry, Technology and Metallurgy, University of Belgrade, Njegoševa 12, P.O. Box 815, 11000 Belgrade, Serbia
¶Institute of Nuclear Sciences 'Vinča', Condensed Matter Physics Laboratory, P.O. Box 522, 11001 Belgrade, Serbia

(*Received 16 September 2011; in final form 19 December 2011*)

A new malonic dihydrazide-based ligand, N',N'^2-bis[(1*E*)-1-(2-quinolyl)methylene]propanedihydrazide (H_2L3), has been prepared and characterized by elemental analysis, IR, ^{13}C NMR, and ^1H NMR spectroscopies. In the reaction of H_2L3 with Ni(II) a binuclear complex has been obtained. The structure of the complex was established by X-ray analysis. Each Ni(II) is coordinated with two NNO donor sets from two ligand molecules in dianionic form ($L3^{2-}$) forming an octahedral geometry. Multiple intramolecular C–H $\cdots$ π (chelate ring) interactions support the molecular geometry of the $[Ni_2(L3)_2]$ complex. The structure of $[Ni_2(L3)_2]$ is compared with those of analogous Ni(II) complexes with pyridine dihydrazone type ligands. Magnetic behavior of the dinuclear complex was studied in temperature range of 2–300 K.

Keywords: Ni(II) complexes; X-ray structure; Intramolecular interactions

1. Introduction

Our studies on d-metal complexes with polydentate *N*-heteroaromatic dihydrazone type ligands have mostly concerned condensation derivatives of 2-acetylpyridine and oxalic or malonic acid dihydrazide [1–4]. The oxalic dihydrazide-based ligand N',N'^2-bis[(1*E*)-1-(2-pyridyl)ethylidene]ethanedihydrazide (H_2L1, scheme 1a) with M(II) ions (M(II) = Cu and Ni) formed complexes which differed considerably in coordination mode of the

*Corresponding author. Email: kka@chem.bg.ac.rs

ISSN 0095-8972 print/ISSN 1029-0389 online
http://dx.doi.org/10.1080/00958972.2012.658778

ligand and the complex nuclearity [5]. Moreover, H_2L1 was often hydrolytically unstable, which resulted in the formation of M(II) complexes (M(II) = Fe [1] and Cu [6]) with 2-acetylpyridine hydrazone. Structurally similar, but more flexible, malonic dihydrazide-based ligand, N',N'^2-bis[(1*E*)-1-(2-pyridyl)ethylidene]propanedihydrazide (H_2L2, scheme 1b), formed with M(II) ions (M(II) = Ni, Zn, and Cd) binuclear complexes of coordination number six $\{[Ni_2(H_2L2)_2](ClO_4)_4$, $[Ni_2(HL2)(H_2L2)](ClO_4)_3$, $[Zn_2(H_2L2)_2](BF_4)_4$ [4]$\}$ or seven $\{[Cd_2(H_2O)_2(H_2L2)_2](ClO_4)_4 \cdot 4H_2O$ [3]$\}$, in which two ligands coordinated the two metal centers in a *bis*-tridentate mode [3, 4]. The coordination of each ligand was achieved by two NNO donor sets which led to the formation of four five-membered chelate rings.

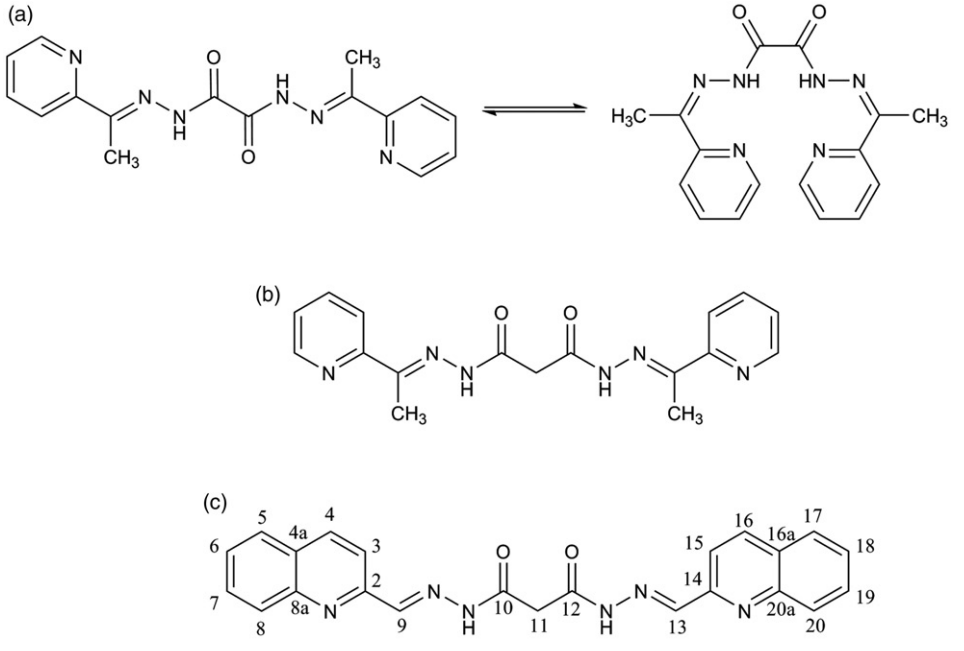

Scheme 1. Polydentate *N*-heteroatomic dihydrazone type ligands: (a) N',N'^2-bis[(1*E*)-1-(2-pyridyl)ethylidene]ethanedihydrazide (H_2L1); (b) N',N'^2-bis[(1*E*)-1-(2-pyridyl)ethylidene]propanedihydrazide (H_2L2); (c) N',N'^2-bis[(1*E*)-1-(2-quinolyl)methylene]propanedihydrazide (H_2L3).

Evaluation of cytotoxic activity of both types of ligands, i.e., H_2L1 and H_2L2 on HeLa cells appeared promising, for these ligands were more active than the other acyl hydrazones of 2-acetylpyridine [3, 7]. The $[Cd_2(H_2O)_2(H_2L2)_2](ClO_4)_4 \cdot 4H_2O$ complex showed a strong dose-dependent activity to B16 melanoma cells and moderate activity to HeLa cells [3].

Encouraged by these results, we have extended our studies to ligands derived from condensation of 2-quinolinecarboxaldehyde and oxalic or malonic acid dihydrazide. Here, we report the synthesis and structural characterization of a new malonic dihydrazide-based ligand, N',N'^2-bis[(1*E*)-1-(2-quinolyl)methylene]propanedihydrazide (H_2L3, scheme 1c) and its Ni(II) complex $[Ni_2(L3)_2] \cdot 3C_2H_5OH \cdot 2H_2O$, and investigate what consequences the replacement of pyridine by quinoline might have on the structure of its metal complex.

2. Experimental

2.1. *Materials*

2-Quinolinecarboxaldehyde (97%), malonic acid dihydrazide (97%), and $Ni(AcO)_2 \cdot 4H_2O$ were obtained from Aldrich. Ethanol and dimethyl sulfoxide were reagent grade and used without purification.

2.2. *Synthesis of N′,N′²-bis[(1E)-1-(2-quinolyl)methylene] propanedihydrazide ($H_2L3 \cdot 3H_2O$)*

Malonic dihydrazide (0.13 g, 1 mmol L^{-1}) was added to a solution of 2-quinolinecarboxaldehyde (0.31 g, 2 mmol L^{-1}) in water (25 mL) and the mixture was refluxed for 3 h. A white solid was filtered off, washed with cold water, and vacuum dried. Elemental analysis: Anal. Calcd for $C_{23}H_{24}N_6O_5$ (%): C, 59.48; H, 5.21; N, 18.09. Found: C, 59.74; H, 5.27; N, 17.98; m.p. (°C) > 210; Yield: 80%. IR (most important bands) (KBr; ν cm^{-1}): 3429 (vs), 2987 (w), 2929 (w), 1710 (s), 1670 (vs), 1598 (m), 1577 (w), 1532 (w), 1500 (w), 1395 (m), 1322 (w), 1305 (w), 1227 (m), 1154 (m), 942 (w), 754 (m), 623 (w), 521 (w), 437 (w), 402 (w). ^{1}H NMR (δ): 4.14 (s, 1 H, C11), 7.61 (t, $J = 7.5$ Hz, 1 H, C6), 7.79 (t, $J = 8.5$ Hz, 1 H, C7), 7.94 (d, $J = 7.5$ Hz, 1 H, C5), 8.03 (d, $J = 8.5$ Hz, 1 H, C8), 8.04 (d, $J = 9.0$ Hz, 1 H, C3), 8.22 (s, 1 H, C9), 8.26 (d, $J = 9.0$ Hz, 1 H, C4), 11.94 (s, 1 H, N3H). ^{13}C NMR (δ): 153.5 (C2 and C14), 117.1 (C3 and C15), 136.5 (C4 and C16), 128.8 (C4a and C16a), 128.0 (C5 and C17), 127.2 (C6 and C18), 130.1 (C7 and C19), 127.7 (C8 and C20), 147.3 (C8a and C20a), 143.5 (C9 and C13), 169.6 (C10 and C12), 41.2 (C11).

2.3. *Synthesis of $[Ni_2(L3)_2] \cdot 3C_2H_5OH \cdot 2H_2O$*

$Ni(OAc)_2 \cdot 4H_2O$ (0.24 g, 1 mmol L^{-1}) was added to a solution of H_2L3 (0.46 g, 1 mmol L^{-1}) in ethanol/DMSO (10 : 1). The reaction mixture was heated at 65°C with stirring for 1 h. After cooling to room temperature, a brown precipitate was filtered off and washed with cold ethanol. Microcrystalline product was purified by vapor diffusion using DMSO solution as an inner solution and ethanol as an outer solvent. Elemental analysis: Anal. Calcd for $C_{52}H_{54}N_{12}Ni_2O_9$ (%): C, 56.35; H, 4.91; N, 15.16. Found: C, 55.25; H, 5.15; N, 15.20; M.p. (°C) = 255; Yield: 75%. IR (most important bands) (KBr; ν cm^{-1}): 3411 (s), 2156 (w), 1642 (w), 1590 (m), 1552 (m), 1488 (vs), 1450 (s), 1432 (m), 1302 (m), 1237 (s), 1085 (vs), 1008 (m), 973 (w), 951 (w), 929 (w), 759 (m), 655 (m), 628 (w), 487 (w), 466 (w). Λ_M (1×10^{-3} mol L^{-1}, DMSO): 0.3 Ω^{-1} cm^2 mol^{-1}, $\mu_{eff}(299\,K) = 1.13\,\mu_B$.

2.4. *Physical measurements*

IR spectra were recorded on a Perkin-Elmer FT-IR 1725X spectrometer using the KBr-pellet technique from 4000 to 400 cm^{-1}. NMR spectra were recorded on a Bruker Avance 500 equipped with broad-band direct probe. All spectra were measured at 298 K. H_2L3 was characterized on the basis of NMR spectroscopy, 1-D (^{1}H, ^{13}C, DEPT), 2-D (COSY-Correlation Spectroscopy and ^{1}H–^{13}C heteronuclear correlation

spectra). Chemical shifts are given on δ scale relative to tetramethylsilane (TMS) as internal standard for ^{1}H and ^{13}C.

Magnetic measurements were performed at 26°C by Evans' method using an MSB-MK1 balance (Sherwood Scientific Ltd.) with $Hg[Co(SCN)_4]$ as calibrant; diamagnetic corrections were calculated from Pascal's constants. Molar conductivities were measured at room temperature (23°C) on a digital conductivity-meter JENWAY-4009.

The temperature dependence of magnetic susceptibility was measured on a powder sample by employing a commercial Quantum Design MPMS-XL-5 SQUID magnetometer from 2 K to 300 K in a 100 Oe magnetic field.

2.5. *X-ray analysis of* $[Ni_2(L3)_2]\cdot 3C_2H_5OH\cdot 2H_2O$

Crystals grown by slow diffusion of ethanol into DMSO were very unstable in air. For X-ray measurements the crystal was mounted in a loop containing some perfluoroether as a protecting agent and flash-cooled on a diffractometer to 130 (1) K. The intensity data were measured with a Xcalibur kappa-geometry diffractometer using graphite monochromated Mo-Kα radiation ($\lambda = 0.71073$ Å) [8] and the temperature of the samples was controlled with an Oxford Instruments Cryosystem cold-nitrogen-gas blower.

The intensity data were corrected for Lp effects as well as for absorption [8]. The structure was solved by direct methods using *SHELXS-97* [9] and refined by least-squares techniques with *SHELXL-97* [10]. The non-hydrogen atoms of the complex were modeled with anisotropic displacement parameters. At the final stages of the refinement it became evident that the crystal structure contains two water molecules and three ethanol molecules in the independent part of the unit cell; the solvent molecules are the source of severe crystal disorder. The disorder model for two of the three ethanol molecules was such that two sites were identified for either one of the carbons with occupancy of 55% and 45%, or the oxygen atom, with occupancy of 80% and 20%. The remaining ethanol was highly disordered, so the proposed disorder model had all atoms distributed over two sites with occupancy of 65% and 35%. At first, these ethanol molecules were refined with positional restraints and with anisotropic displacement parameters for atoms constituting the major component of the disorder while atoms constituting the minor component were refined isotropically. Nevertheless, the proposed disorder model was still unsatisfactory. Therefore, we have removed all disordered solvent molecules from the model and used *SQUEEZE* [11] program to account for the presence of these solvent molecules. The program indicated the presence of a void around 000 of the volume of *ca* 1303 Å^3 containing 292 electrons which resulted from the removal of the disordered one water and three ethanol molecules. Hence, the provided atom list does not contain atoms of these disordered solvent molecules. Hydrogen atoms connected to carbons were placed in calculated positions and included in the refinement using a riding model, with C–H distances of 0.95 Å for C(aromatic)–H and 0.99 Å for methylene groups with $U_{iso}(H) = 1.2U_{eq}(C)$. Hydrogen atoms belonging to a not-disordered water have been located on a difference Fourier and refined as riding with $U_{iso}(H) = 1.2U_{eq}(O)$. Molecular plots were obtained with *XP* [12] and *Mercury* [13] programs. Selected crystal data are listed in table 1 and selected bond lengths and valence angles in table 2.

Table 1. Crystal data for $[Ni_2(L3)_2]\cdot 3C_2H_5OH\cdot 2H_2O$.

Crystal data	
Chemical formula	$C_{46}H_{32}N_{12}Ni_2O_4\cdot 3(C_2H_6O)\cdot 2(H_2O)$
Formula weight	1108.49
Temperature (K)	130
Crystal system	Monoclinic
Space group	$P2_1/n$
Unit cell dimensions (Å, °)	
a	14.8617(8)
b	20.0099(11)
c	17.4533(10)
β	92.918(5)
Volume (Å^3), *Z*	5183.6(5), 4
Radiation type	Mo-Kα
Absorption coefficient (mm^{-1})	0.80
Crystal size (mm^3)	$0.50\times 0.10\times 0.05$
Data collection	
Diffractometer	Xcalibur, Eos diffractometer
Scan method	*ω* scans
Absorption correction	Multi-scan
T_{min} and T_{max}	0.747 and 1.000
Number of measured, independent, and observed $[I > 2\sigma(I)]$ reflections	31,605, 9138, and 4928
R_{int}	0.081
Refinement	
$R[F^2 > 2\sigma(F^2)]$, $wR(F^2)$, *S*	0.045, 0.098, 0.81
Number of reflections	9138
Number of parameters	586
H-atom treatment	H-atom parameters constrained
$\Delta\rho_{max}$ and $\Delta\rho_{min}$ (e Å^{-3})	0.55 and –0.40

2.6. *CSD search*

A Cambridge Structural Database (CSD) [14] search (version 5.32, November 2010 + 1 update) was performed using the *ConQuest* program [15] to extract all structures containing any metal coordinated to quinoline and at the same time chelated by ethane-1,2-diimine, and displaying parameters favorable for C–H $\cdots\pi$ interactions, i.e., the H $\cdots$ C_g (C_g = center of gravity) distance less than 3.0 Å and the C–H $\cdots$ C_g angle not less than 100°. We have obtained 10 hits listed in table 3. For further interpretation of the crystallographic data, we have used the exported cif files for all 10 structures and the *PLATON* [11] program for calculations.

3. Results and discussion

3.1. *General*

N′,*N*′^{2}-bis[(1 *E*)-1 -(2-quinolyl)methylene]propanedihydrazide (H_2L3) was obtained by condensation of 2-quinolinecarboxaldehyde with the dihydrazide of malonic acid in a

Table 2. Selected bond lengths and valence angles.

Ni1–N1	2.157(3)	Ni2–N3	2.145(3)
N1–C1	1.328(4)	N3–C31	1.329(4)
C1–C10	1.471(5)	C31–C30	1.465(5)
N11–C10	1.277(4)	N31–C30	1.286(4)
Ni1–N11	1.979(3)	Ni2–N31	1.989(3)
Ni1–N2	2.163(3)	Ni2–N4	2.136(3)
N2–C21	1.343(4)	N4–C41	1.332(4)
C20–C21	1.457(5)	C41–C40	1.459(5)
N21–C20	1.279(4)	N41–C40	1.276(4)
Ni1–N21	1.983(3)	Ni2–N41	1.989(3)
Ni1–O1	2.081(2)	Ni2–O3	2.061(2)
O1–C11	1.263(4)	O3–C16	1.263(4)
N12–C11	1.347(4)	N32–C16	1.334(4)
N11–N12	1.381(4)	N31–N32	1.364(4)
N11–Ni1	1.979(3)	N31–Ni2	1.989(3)
Ni1–O2	2.084(2)	Ni2–O4	2.102(2)
O2–C14	1.265(4)	O4–C13	1.261(4)
N22–C14	1.340(4)	N42–C13	1.340(4)
N21–N22	1.378(4)	N41–N42	1.376(4)
N21–Ni1	1.983(3)	N41–Ni2	1.989(3)
N11–Ni1–N1	78.56(12)	N31–Ni2–N3	78.48(12)
C1–N1–Ni1	109.7(2)	C31–N3–Ni2	110.3(2)
N1–C1–C10	117.3(3)	N3–C31–C30	116.2(3)
N11–C10–C1	115.1(3)	N31–C30–C31	116.1(3)
C10–N11–Ni1	118.9(3)	C30–N31–Ni2	117.2(3)
N21–Ni1–N2	78.41(11)	N41–Ni2–N4	78.09(11)
C21–N2–Ni1	109.8(2)	C41–N4–Ni2	110.8(2)
N2–C21–C20	116.8(3)	N4–C41–C40	116.4(3)
C21–C20–N21	116.1(3)	N41–C40–C41	115.5(3)
C20–N21–Ni1	118.8(2)	C40–N41–Ni2	118.4(2)
N11–Ni1–O1	76.32(11)	N31–Ni2–O3	76.68(11)
C11–O1–Ni1	111.0(2)	C16–O3–Ni2	110.0(2)
O1–C11–N12	125.3(3)	O3–C16–N32	126.9(3)
C11–N12–N11	107.5(3)	C16–N32–N31	107.2(3)
N12–N11–Ni1	119.4(2)	N32–N31–Ni2	118.8(2)
N21–Ni1–O2	76.97(10)	N41–Ni2–O4	76.37(10)
C14–O2–Ni1	109.8(2)	C13–O4–Ni2	110.1(2)
O2–C14–N22	125.7(3)	O4–C13–N42	125.7(3)
C14–N22–N21	108.5(3)	C13–N42–N41	108.5(3)
N22–N21–Ni1	118.1(2)	N42–N41–Ni2	118.7(2)

molar ratio 2 : 1 in water (pH ~ 4.5). The chemical composition of the ligand was confirmed by elemental analysis and its structure was determined by ^{13}C and ^{1}H NMR spectroscopies. In the reaction of H_2L3 with $Ni(OAc)_2$ in EtOH/DMSO solution (10 : 1) $[Ni_2(L3)_2] \cdot 3C_2H_5OH \cdot 2H_2O$ was obtained. The elemental analysis data and the molar conductivity results suggest that complex is neutral and binuclear. Ligand (H_2L3) is soluble in DMSO, DMF, and hot EtOH and $[Ni_2(L3)_2] \cdot 3C_2H_5OH \cdot 2H_2O$ is insoluble. The IR spectral data of the complex revealed that both hydrazide moieties of the ligand are deprotonated, as evidenced by the disappearance of the amide band I [ν(C=O)] at 1670 cm^{-1}, clearly visible in the IR spectrum of the ligand. $[Ni_2(L3)_2] \cdot 3C_2H_5OH \cdot 2H_2O$ is paramagnetic with possible antiferromagnetic (AF) characteristics as suggested by the magnetic susceptibility at room temperature (the value of magnetic moment per metal center is $\mu = 0.798\,\mu_B$) [16]. Further experiments to evaluate the magnetic behavior of

Table 3. Intramolecular $C8_{quinoline}$–H ··· π(chelate ring: M–$N_{quinoline}$–C–C–N_{imine}–) interaction parameters for $[Ni_2(L3)_2]$ and the corresponding complexes available from the CSD [14]. C_g is the centroid of chelate ring and γ is the angle between H ··· C_g line and the normal to the chelate ring.

	H ··· C_g (Å)	H ··· (ring plane) (Å)	C–H ··· C_g (°)	γ (°)	Reference
DIRYAF[a,b] Ni(II)					[19]
	2.55	2.52	144	9	
	2.46	2.40	145	12	
KIHSEA[a,b] Ni(II)					[20]
	2.66	2.51	137	20	
	2.66	2.56	144	16	
METLUT[a,b] Ni(II)					[21]
	2.68	2.47	140	22	
	2.66	2.48	141	21	
XULQUR[a,b] Co(III)					[22]
	2.54	2.37	134	21	
	2.56	2.39	132	21	
$[Ni_2(L3)_2]\cdot 3C_2H_5OH\cdot 2H_2O$[b,c]					This work
CH–(chelate ring)					
C8H8A–(Ni1N2C21C20N21)	2.51	2.47	144	11	
C28H28A–(Ni1N1C1C10N11)	2.60	2.54	143	12	
C38H38A–(Ni2N4C41C40N41)	2.52	2.51	146	5	
C48H48A–(Ni2N3C31C30N31)	2.61	2.57	144	10	
KEMZEI[b,c] Zn(II)					[23]
	2.67	2.65	147	6	
	2.90	2.67	146	23	
KAGSUH[c,d] Cu(I)					[24]
	2.95	2.72	145	23	
	3.01	2.76	144	23	
	2.90	2.67	146	23	
MIVXUL[b,e] Zn(II)					[25]
	2.53	2.51	149	7	
	2.74	2.64	143	15	
	2.65	2.60	146	11	
	2.77	2.69	146	14	
MIVYAS[b,e] Co(II)					[25]
	2.64	2.59	142	12	
	2.50	2.47	144	8	
	2.56	2.54	144	5	
	2.73	2.68	144	11	
RINXIW[b,f] Mn(II)					[26]
	2.66	2.59	150	13	
	2.68	2.64	150	9	
	2.63	2.62	151	6	
	2.69	2.60	151	15	
BOYJUV[b,g] Mn(II)					[27]
	2.80	2.55	146	24	

[a]Mononuclear complexes; [b]octahedral complexes; [c]binuclear complexes; [d]tetrahedral complexes; [e]hexanuclear complexes; [f]nonanuclear complexes; [g]hexadecanuclear structure.

the material at low temperatures are in progress and will aim at a concise picture of the coupling in the solid phase. The structure of the complex was determined by single-crystal X-ray analysis.

3.2. *Description of the crystal structure*

An *ORTEP* drawing of the binuclear $[Ni_2(L3)_2]$ complex is presented in figure 1, where the numbering scheme adopted for the respective atoms is also given. Selected bond

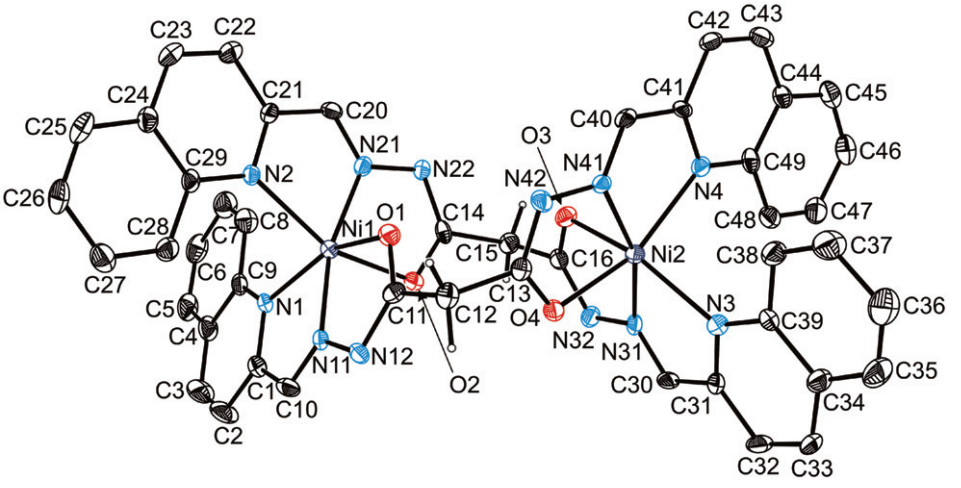

Figure 1. *ORTEP* drawing of $[Ni_2(L3)_2]$. Atomic displacement ellipsoids for non-H atoms are drawn at 40% probability. Hydrogen spheres are drawn in an arbitrary scale. Hydrogen atoms bonded to the C_{sp}^2 carbons are not shown.

lengths and valence angles are listed in table 2. In the investigated binuclear complex each Ni(II) is coordinated with two sets of NNO donors from two di-deprotonated molecules ($L3^{2-}$) forming a distorted octahedron. One of the measures of the octahedral strain is average ΔO_h value, defined as the mean deviation of 12 octahedral angles from ideal 90°. The distorted octahedra formed around Ni(1) and Ni(2) exhibit average ΔO_h values of 9.2° and 9.4°, respectively. Similar degree of octahedral distortion has been observed previously [4] in binuclear complex cations $[Ni_2(H_2L2)_2]^{4+}$ and $[Ni_2(HL2)(H_2L2)]^{3+}$, for which the reported average ΔO_h values were 8.9° to 9.6°. Each $L3^{2-}$ coordinates to two Ni(II) centers in a bis-tridentate mode, thereby forming four five-membered chelate rings. The planes formed by the five atoms constituting the two O,N,N-chelates coordinated to one metal center are mutually perpendicular with dihedral angles of 86.2° and 87.9°. A twelve-membered macrocyclic ring (Ni–O–C–CH_2–C–O–)$_2$ with the intramolecular Ni ··· Ni separation of 6.0165(7) Å makes the core of the $[Ni_2(L3)_2]$ complex. The overall geometry of the investigated complex is comparable with that observed in the structurally related binuclear complexes $[Ni_2(H_2L2)_2](ClO_4)_4$ [4], $[Ni_2(HL2)(H_2L2)](ClO_4)_3$ [4], $[Zn_2(H_2L2)_2](BF_4)_4$ [4], and $[Cd_2(H_2O)_2(H_2L2)_2](ClO_4)_4 \cdot 4H_2O$ [3]. In all these complexes, the same bis-tridentate coordination of the malonic dihydrazide-based ligand H_2L2 and the formation of the twelve-membered macrocyclic ring (M(II)–O–C–CH_2–C–O–)$_2$ (M(II) = Ni, Zn, and Cd) have been observed. In octahedral binuclear Ni(II) complexes the two NNO chelating systems were mutually perpendicular, as evidenced by values of the dihedral angles of 83.6° and 82.5° in $[Ni_2(H_2L2)_2](ClO_4)_4$, and 83.7° and 85.6° in $[Ni_2(HL2)(H_2L2)](ClO_4)_3$ [4] but in the seven-coordinate $[Cd_2(H_2O)_2(H_2L2)_2](ClO_4)_4 \cdot 4H_2O$ these angles were only 70° and 75° [3].

The mean value of the four bond angles around the deprotonated hydrazone nitrogen atoms (N12, N22, N32, and N42) in $[Ni_2(L3)_2]$ is 107.9(6)°, being indicative of a full deprotonation of the ligand. For comparison, the values of the bond angles around the

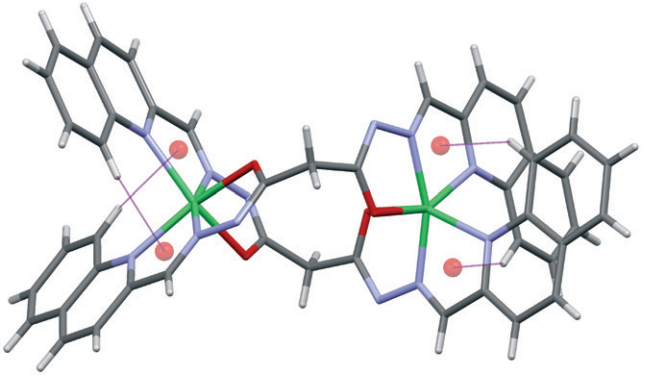

Figure 2. C–H···π intramolecular interactions (thin lines) involving C8–H(quinoline) and M–$N_{quinoline}$–C–C–N_{imine} chelate ring. Spheres denote the centers of gravity of the chelate rings.

protonated nitrogen atoms in $[Ni_2(H_2L2)_2](ClO_4)_4$ and $[Ni_2(HL2)(H_2L2)](ClO_4)_3$ were much higher, ranging from 112.7(5)° to 116.0(5)° [4]. A striking difference between the investigated $[Ni_2(L3)_2]$ complex and previously reported $[Ni_2(H_2L2)_2](ClO_4)_4$ and $[Ni_2(HL2)(H_2L2)](ClO_4)_3$ is the reverse relationship between the lengths of the Ni–N_{aryl} and Ni–$O_{amidate}$ bonds, situated *trans* to each other. In $[Ni_2(L3)_2]$ the mean Ni–$N_{quinoline}$ bond [2.15(1) Å] is longer than the mean Ni–O bond [2.08(2) Å], while the mean Ni–$N_{pyridine}$ and Ni–O bonds in $[Ni_2(H_2L2)_2](ClO_4)_4$ and $[Ni_2(HL2)(H_2L2)](ClO_4)_3$ were 2.08(1) and 2.10(1) Å, respectively. At the same time the Ni–N_{imine} bond length remains unaffected and its average value sums to 1.985(5) Å. The apparent shortening of the Ni–O bond in the reported $[Ni_2(L3)_2]$ complex is accompanied by lengthening of the proximal C–O bond (mean value 1.264(3) Å) which presumably reflects a delicate interplay between the enolic *versus* ketonic character of this bond in the fully deprotonated *versus* partially deprotonated ligands. In the fully deprotonated ligand the C–O bond has more enolic structure, while in the monoprotonated ligand it reveals more ketonic character, the corresponding mean values for this bond length being 1.270 (4) *versus* 1.240 (8) Å. Combined with the changes in the C–O and Ni–O bond lengths are the simultaneous changes in the Ni–$N_{aromatic}$ bond lengths situated *trans* with respect to the Ni–O bonds. To verify whether the observed alternating shortening and lengthening of the C–O, Ni–O, and Ni–$N_{aromatic}$ bond lengths is not incidental, we have analyzed a pair of Ni(II) semicarbazone complexes differing in the degree of ligand deprotonation [17, 18]. In the Ni(II) complex with the fully deprotonated ligand the mean values of the Ni–N, Ni–O, and C–O distances were 2.115(10), 2.093(3), and 1.266(1) Å, while in its counterpart, i.e., the Ni(II) complex with a monodeprotonated ligand, these values were 2.098(8), 2.137(6), and 1.244(4) Å, respectively. The provided example confirms that there is indeed a relationship between the tautomeric form of the hydrazone ligand and the Ni–N(aromatic) bond length.

A closer look at the shape of $[Ni_2(L3)_2]$ reveals a nearly perpendicular (or T-shaped) orientation of a quinoline six-membered carbon ring of one ligand with respect to the metal chelate quinolineimine ring of the other ligand. Such orientation is indicative of the presence of intramolecular C–H $\cdots$ π interactions. The observed intramolecular CH $\cdots$ $\pi_{chelate\ ring}$ interactions between aryl C8–H bonds and Ni(II)–$N_{quinoline}$–C–C–N_{imine} chelate rings are illustrated in figure 2. As can be seen from this figure, there are

four pairs of such interactions in one complex molecule, so their effect on complex geometry might be substantial. Geometrical parameters describing these interactions are presented in table 3 together with the corresponding data for other metal complexes [19–27] obtained while searching the CSD [14]. It follows from this table that the intramolecular CH $\cdots\pi$ interaction to the Ni(II) ethane-1,2-diimine chelate ring is common in complexes containing M–$N_{quinoline}$–C–C–N_{imine} fragments. The presence of such interactions often escapes the authors' attention, despite a steady increase in the number of papers reporting the importance of CH $\cdots\pi$ hydrogen bonds in the crystal structure of metal complexes [28 and references therein]. A possibility of the presence of C–H $\cdots\pi$ interactions between chelate and aryl rings in the crystal structures of square planar transition metal complexes has recently been discussed by Sredojević and co-workers [29], and this type of interaction has also been reported to exist in bis(pyridine-2,6-diimine)Ru^{II} complexes [30]. Examination of the complex geometry in relation to the data presented in table 3 did not reveal any clear relationship with the C–H $\cdots\pi$ interactions. It seems, therefore, that the presence of such interactions mostly results from the quinoline ring being part of the relatively rigid metal complex. The quinoline ring is clearly a much larger aromatic component than the pyridine ring normally present in this ligand type, and it is reasonable to assume that, as the ligands approach each other in the typical meridional arrangement, the C–H(quinoline) interactions with the delocalized π-electrons of the ethane-1,2-diimine nickel chelate ring become possible.

Intermolecular hydrogen bonds include solvent molecules (ethanol and water) as hydrogen-bond donors to either themselves or to the deprotonated amide nitrogen atoms (N12, N22, and N24). Weaker C–H $\cdots$ N32 hydrogen bonds complement hydrogen-bond interactions with the deprotonated amide nitrogen atoms. No meaningful discussion of H-bonding can be made because of the disorder of the solvent molecules which eventually have been removed from the atom list using a SQUEEZE procedure inserted in PLATON [11].

3.3. *Magnetic measurement*

The data were corrected for the contributions of the sample holder and for the diamagnetism of the sample estimated from Pascal's constants. Magnetic data are shown in figure 3, where inverse magnetic susceptibility ($1/\chi_A$) per mol of Ni^{2+} and effective magnetic moment (μ_{eff}) per Ni^{2+} *versus* T are presented.

Inverse magnetic susceptibility shows linear dependence on temperature. For $T > 100\,K$ fitting to the Curie–Weiss law, $\chi_A = C\ (T - \theta)^{-1}$, gives $\theta = -8\,K$ and $C = 1.14\ cm^3\ mol^{-1}\ K^{-1}$. Negative value of Weiss constant indicates the existence of weak AF interaction which exists between two Ni^{2+} ions (intradimer). This interaction, together with the interdimer interactions and/or zero-field splitting effect, causes deviation from the linear behavior at low temperatures (figure 3). The effective magnetic moment $\mu_{eff} = 3.0\,\mu_B$, obtained from Curie constant C, is slightly higher than the spin-only value for Ni^{2+} ($\mu_{eff} = 2.83\,\mu_B$).

As shown in the same figure, upon cooling, magnetic moment slowly decreases from $\mu_{eff} = 2.98\,\mu_B$ at 300 K to $\mu_{eff} = 2.80\,\mu_B$ at 19 K due to weak AF interaction and this decrease is more pronounced at lower temperatures when interdimer interaction could also give their contribution. Temperature dependence of effective magnetic moment

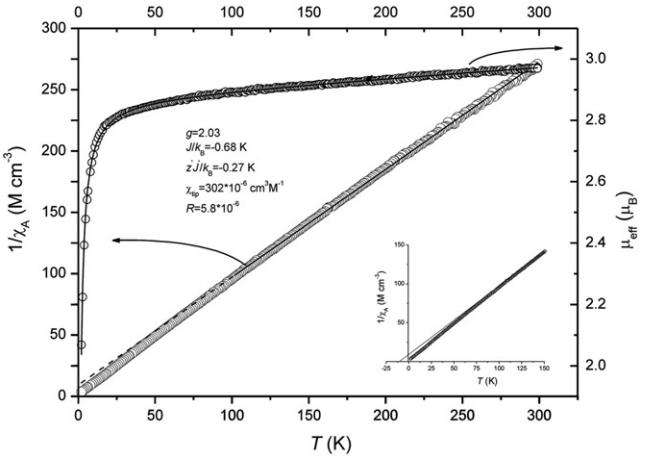

Figure 3. Temperature dependence of inverse magnetic susceptibility (open circles) and Curie–Weiss plot (solid and dashed lines). Effective magnetic moment *vs.* temperature (open circle) and fit to equation (1) (solid line). Inset: Deviation from Curie–Weiss plot at low temperatures.

$\mu_{\text{eff}}(T)$ was analyzed by the Ginsberg model [31] based on Heisenberg Hamiltonian which includes exchange between spins, effect of external field as well as interdimer interaction in the molecular field approximation. Zero-field splitting effects were not explicitly taken into consideration since it is well-known that these effects can be masked by interdimer interactions and is more important for ferromagnetic coupling [32]. The last equation can be written in the following form:

$$\mu_{\text{eff}} = \sqrt{[3g^2F(J,T)]/[1 - 4z'J'F(J,T)/k_{\text{B}}T] + 8\chi_{\text{TIP}} \cdot T},$$
$$F(J,T) = [1 + 5e^{4J/k_{\text{B}}T}]/[3 + 5e^{4J/K_{\text{B}}T}] + e^{-2J/k_{\text{B}}T}. \quad (1)$$

In this equation g and k_{B} have their usual meaning, J is exchange integral for the intradimer interaction between nickel ions, χ_{TIP} is temperature independent paramagnetism, and $z'J'$ is interdimer exchange integral in the molecular field approximation. The best fit values were $g = 2.03$, $J/k_{\text{B}} = -0.68$ K, $z'J'/k_{\text{B}} = -0.27$ K, and $\chi_{\text{TIP}} = 302 \times 10^{-6}$ cm^3 mol^{-1} with $R = 5.8 \times 10^{-6}$ [$R = \sum(\mu_{\text{eff}}^{\text{obs}} - \mu_{\text{eff}}^{\text{calc}})^2/(\sum \mu_{\text{eff}}^{\text{obs}})^2$]; $\mu_{\text{eff}}(T)$ curve shows an excellent fit to the experimental data in the entire temperature range measured. In the high temperature limit equation (1) tends to $\mu_{\text{eff}}\,(T \to \infty) = \sqrt{2}\,g$ [31] which is in accord with the obtained value $\mu_{\text{eff}}\,(T = 300\text{ K}) = 2.98\,\mu_{\text{B}}$. The negative value for J indicates mild antiferromagnetism, which is small and close to $z'J'$, due to the relatively large pathway between two Ni^{2+} ions belonging to the same dimer.

4. Conclusion

Unlike the previously reported metal complexes with pyridine dihydrazone type ligands, their quinoline analog, whose synthesis and structure is reported in this article, displays a pronounced tendency to form multiple CH···π(metal chelate ring) interactions stimulated by the presence of quinoline rather than more commonly used pyridine

moiety. The contribution from multiple weak CH···π(metal chelate ring) interactions should not be ignored in the interpretation of the experimental results, despite their extreme weakness. Magnetic data were analyzed by means of Heisenberg Hamiltonian which includes the intra and interdimer interactions as well as the effect of external magnetic field. Due to long Ni^{2+}–Ni^{2+} pathway, very weak intradimer AF exchange integral ($J/k_B = -0.68$ K) was found which is comparable with effective interdimer interactions.

Supplementary material

CCDC 813890 contains the supplementary crystallographic data for $[Ni_2(L3)_2] \cdot 3C_2H_5OH \cdot 2H_2O$ with disordered solvent molecules included while CCDC 858072 contains the supplementary crystallographic data for $[Ni_2(L3)_2] \cdot 3C_2H_5OH \cdot 2H_2O$ with disordered solvent molecules (one water and three ethanol molecules) removed from the atomic list. These data can be obtained free of charge *via* http://www.ccdc.cam.ac.uk/conts/retrieving.html, or from the Cambridge Crystallographic Data Centre, 12 Union Road, Cambridge CB2 1EZ, UK; Fax: (+44) 1223-336-033; or E-mail: deposit@ccdc.cam.ac.uk.

Acknowledgments

This work was funded in part by the Ministry of Science and Technological Development of the Republic of Serbia (Project No. IIO 172055).

References

[1] K. Anđelković, D. Sladić, A. Bacchi, G. Pelizzi, N. Filipović, M. Rajković. *Transition Met. Chem.*, **30**, 243 (2005).
[2] G.N. Kaluđerović, R.O.M. Eshkourfu, S. Gómez-Ruiz, D. Mitić, K. Anđelković. *Acta Cryst. Sect. E*, **66**, o904 (2010).
[3] N. Filipović, A. Bacchi, M. Lazić, G. Pelizzi, S. Radulović, D. Sladić, T. Todorović, K. Anđelković. *Inorg. Chem. Commun.*, **11**, 47 (2008).
[4] T. Todorović, U. Rychlewska, B. Warżajtis, D. Radanović, N. Filipović, I. Pajić, D. Sladić, K. Anđelković. *Polyhedron*, **28**, 2397 (2009).
[5] S. Sen, C.R. Choudhury, P. Talukder, S. Mitra, M. Westerhausen, A.N. Kneifel, C. Desplanches, N. Daro, J.P. Sutter. *Polyhedron*, **25**, 1271 (2006).
[6] T.L. Kelly, V.A. Milway, H. Grove, V. Niel, T.S.M. Abedin, L.K. Thompson, L. Zhao, R.G. Harvey, D.O. Miller, M. Leech, A.E. Goeta, J.A.K. Howard. *Polyhedron*, **24**, 807 (2005).
[7] M. Lazić, S. Radulović, T. Todorović, D. Sladić, Ž. Tešić, K. Anđelković. *Mater. Sci. Forum*, **518**, 513 (2006).
[8] *CrysAlis CCD and CrysAlis RED software (Version 1.171)*, Oxford Diffraction, Oxfordshire, England (2000).
[9] G.M. Sheldrick. *Acta Cryst. Sect. A*, **46**, 467 (1990).
[10] G.M. Sheldrick. *Acta Cryst. Sect. A*, **64**, 112 (2008).
[11] A.L. Spek. *PLATON, A Multipurpose Crystallographic Tool*, Utrecht University, Utrecht, The Netherlands (2010).
[12] *XP*, Siemens Analytical X-ray Instruments, Inc., Madison, WI, USA (1990).

[13] I.J. Bruno, J.C. Cole, P.R. Edgington, M. Kessler, C.F. Macrae, P. McCabe, J. Pearson, R. Taylor. *Acta Cryst. Sect. B*, **58**, 389 (2002).
[14] F.H. Allen. *Acta Cryst. Sect. B*, **58**, 380 (2002).
[15] F.H. Allen, J.E. Davies, J.J. Galloy, O. Johnson, O. Kennard, C.F. Macrae, E.M. Mitchell, G.F. Mitchell, J.M. Smith, D.G. Watson. *J. Chem. Inf. Comput. Sci.*, **31**, 187 (1991).
[16] S.Y. Zhang, Y. Li, W. Li. *Inorg. Chim. Acta*, **362**, 2247 (2009).
[17] J. Zhou, Z.F. Chen, X.W. Wang, Y.S. Tan, H. Liang, Y. Zhang. *Acta Cryst. Sect. E*, **60**, m568 (2004).
[18] E.R. Garbelini, M. Hörner, V.F. Giglio, A.H. da Silva, A. Barison, F.S. Nunes. *Z. Anorg. Allg. Chem.*, **635**, 1236 (2009).
[19] E. Manoj, M.R.P. Kurup. *Polyhedron*, **27**, 275 (2008).
[20] T. Todorović, A. Bacchi, N. Juranić, D. Sladić, G. Pelizzi, T. Božić, N. Filipović, K. Anđelković. *Polyhedron*, **26**, 3428 (2007).
[21] M.A. Ali, A.H. Mirza, F.H. Bujang, M.H.S.A. Hamid, P.V. Bernhardt. *Polyhedron*, **25**, 3245 (2006).
[22] T.R. Todorović, A. Bacchi, D.M. Sladić, N.M. Todorović, T.T. Božić, D.D. Radanović, N.R. Filipović, G. Pelizzi, K.K. Anđelković. *Inorg. Chim. Acta*, **362**, 3813 (2009).
[23] D.Y. Wu, L.X. Xie, C.L. Zhang, C.Y. Duan, Y.G. Zhao, Z.J. Guo. *Dalton Trans.*, 3528 (2006).
[24] G.K. Patra, I. Goldberg. *New J. Chem.*, **27**, 1124 (2003).
[25] C. He, Z. Lin, Z. He, C. Duan, C. Xu, Z. Wang, C. Yan. *Angew. Chem. Int. Ed.*, **47**, 877 (2008).
[26] S.K. Dey, T.S.M. Abedin, L.N. Dawe, S.S. Tandon, J.L. Collins, L.K. Thompson, A.V. Postnikov, M.S. Alam, P. Muller. *Inorg. Chem.*, **46**, 7767 (2007).
[27] L.N. Dawe, K.V. Shuvaev, L.K. Thompson. *Inorg. Chem.*, **48**, 3323 (2009).
[28] O. Takahashi, Y. Kohno, M. Nishio. *Chem. Rev.*, **110**, 6049 (2010).
[29] D. Sredojević, G.A. Bogdanović, Z.D. Tomić, S.D. Zarić. *CrystEngComm*, **9**, 793 (2007).
[30] Y. Jiang, C. Xi, Y. Liu, J. Niclós-Gutiérrez, D. Choquesillo-Lazarte. *Eur. J. Inorg. Chem.*, 1585 (2005).
[31] A.P. Ginsberg, R.L. Martin, R.W. Brookes, R.C. Sherwood. *Inorg. Chem.*, **11**, 2884 (1972).
[32] E. Berti, A. Caneschi, C. Daiguebonne, P. Dapporto, M. Formica, V. Fusi, L. Giorgi, A. Guerri, M. Micheloni, P. Paoli, R. Pontellini, P. Rossi. *Inorg. Chem.*, **42**, 348 (2003).